SUPPORTING INFORMATION

Phenotypic Screening with Oleaginous Microalgae Reveals Modulators of Lipid Productivity

Annaliese K. Franz*, Megan A. Danielewicz, Diana M. Wong, Lisa A. Anderson, Jordan R. Boothe

Department of Chemistry, University of California, Davis, CA 95616

Table of contents

I. Microalgae Cultures and Screening Compounds

Microalgae strains and culture maintenance. Microalgae species utilized for this study were purchased from the UTEX Culture Collection of Algae at the University of Texas, Austin USA (*Phaeodactylum tricornutum* UTEX B2089, *Nannochloropsis oculata* UTEX LB2164, *Nannochloris sp*. UTEX LB2055) and the Provasoli-Guillard National Center for Marine Algae and Microbiota (NCMA), East Booth Bay, Maine [formerly, the Center for the Culture of Marine Phytoplankton at the Bigelow Laboratory for Ocean Sciences (CCMP)] (*Nannochloropsis salina* CCMP 537). *P. tricornutum* and *N. salina* were grown in F/2 medium (prepared from CCMP protocol) while *N. oculata* and *Nannochloris sp*. were cultured in Erdschreiber's medium (prepared as indicated by UTEX media protocols). Stock cultures were grown in 500-mL Erlenmeyer flask with ventilated Bugstopper caps (Whatman) aerated by orbital shaking (Thermo Scientific MAXQ 2000) at a constant speed of 150 rpm or in 2-L bottles Corning Pyrex media bottles (Corning 1395-2L) using stirring (IKA mini) with air bubbling (Petco Air Pump). Incoming air was sterile filtered by Polyvent 4 disposable filters (Whatman). Stock cultures were maintained at 22 ± 3 °C with a 16:8 hour light/dark cycle.

Microalgae stock cultures. All materials for assay experiments were autoclaved before each use to maintain axenic microalgae cultures for screening. Microalgae species are verified for axenicity using a Nikon Eclipse TS-100 light microscope (Nikon, Japan) before each experiment. For each microplate, 10 mL of diluted microalgae stock was prepared by diluting a stationary phase culture to 0.075 absorbance units with appropriate media without sodium bicarbonate supplementation. Diluted stock solutions are made immediately prior to use for consistency and optimal plate growth. Cell density was measured on a Thermo Scientific Genesys 10S Vis Spectrophotometer (ThermoFisher, San Jose), using a 1-mL cuvette at 680 nm.

Compound selection and preparation of stock solutions. Compounds were selected based on examples of previously reported biological activity (e.g. for yeast and mammalian cells) and were ordered from the following vendors: Fisher BioReagents, Sigma Aldrich, Cayman Chemicals, ChromaDex, Promega, MP Biomedicals, EMD Millipore Chemicals, Tocris Cookson, Axxora LLC, Acros Organics, Cell Signaling Technology, Andwin Scientific, LC Laboratories, Research Products International Corp, Enzo Life Sciences, TCI America, Alfa Aesar, and Supelco (Table S1). Compounds were stored under advised conditions after purchasing from the manufacturer to ensure quality retention. Stock solutions at 10 mM in DMSO were prepared in amber glass vials and stored in the dark at -20°C. To prevent cross contamination during screening, individual compounds were added to separate wells in a PCR plate and organized using a pre-made plate map. Serial dilutions used in the secondary screening were diluted by rows within the same PCR plates. Dilutions and compounds were transferred manually using a multi-channel pipet. All plates were sealed with aluminum plate seals and stored at -20°C. A plate map was used to keep track of each compound in the microplate well based on molecule name, collection number, and CAS number.

Table S1. Compounds, Vendors, and Known Biological Activity

Molecule	Compound class and bioactivity[a]	Catalog #	Vendor
Abscisic acid	Plant growth hormone (agonist of antioxidant response element at 37.6 μM)	190673	MP Biomedicals
Acetaminophen	Analgesic, inhibitor of COX (arachidonate 15-LO, IC_{50} = 28.38 μM)	A5000	Sigma Aldrich
AG 82	Inhibitor of protein tryrosine kinase (EGFR tyrosine kinase, IC_{50} = 3 μM)	658400	EMD Millipore Chemicals
AICAR	Activator of AMPK, inhibitor of fatty acid and sterol synthesis (0.5 mM), inactivates HMG-CoA reductase in rat hepatocytes, inhibitor of insulin-stimulated glucose uptake (0.5 mM), and inhibitor of NF κ B and C/EBP pathways	A9978	Cayman Chemical
Aloisine A	Inhibitor of CDKs (IC_{50} = 150 nM, 120 nM, 400 nM, and 200 nM for Cdk1/cyclin B, Cdk2/cyclin A, Cdk2/cyclin E, and Cdk5/p25, respectively, GSK (GSK-3, IC_{50} = 500 nM and 1.5 μM for GSK-3 α , GSK-3 β , respectively), and c-Jun N-terminal kinase (IC_{50} = ~ 3 - 10 μM)	128125	EMD Millipore Chemicals
Apigenin	Inhibitor of MAPK activity, PKC-like activity	178278	EMD Millipore Chemicals
Arctigenin	Plant lignan, antiviral and antitumor activity	50810264	Tocris Cookson
Atrazine	Herbicide	49085	Supelco
Baicalein	Anti-inflammatory, anti-thrombotic, anti-proliferative and anti-mitogenic activity, inhibitor of 12-LO (IC_{50} = 0.64 μM) and 15-LO (IC_{50} = 1.6 μM)	BML-EI106	Axxora
6-Benzylaminopurine	Cytokinin, plant growth regulator	22641	Acros Organics
Bisindolylmaleimide	Inhibitor of kinases (PKC, K_i = 10 nM; PKA, K_i = 2 μM)	270-049-M001	Axxora
Bohemine	Inhibitor of CDK (IC_{50}= 1 μM)	203600	EMD Millipore Chemicals
BPDQ (4-[(3-bromophenyl)amino]-6,7-diaminoquinazoline)	Inhibitor of the tyrosine kinase activity of the EGFR (IC_{50} = 120 pM)	203697	EMD Millipore Chemicals
BPIQ-II	Inhibitor of the tyrosine kinase activity of the EGFR (IC_{50} = 8 pM)	203704	EMD Millipore Chemicals
Butein	Plant polyphenol, inhibitor of the tyrosine kinase activity of the EGFR (IC_{50} = 65 μM)	203987	EMD Millipore Chemicals
BHA (Butylated hydroxyaniaole)	Antioxidant, DPPH free radical scavenging activity (IC_{50} = 43 μM)	2101159	MP Biomedicals
Caffeic acid	Plant phenolic compound with anti-tumor, antiviral, antioxidant and anti-inflammatory activity, inhibitor of 5- and 12-LO (5-LO, IC_{50} = 3.7 μM)	270-231	Axxora
cAMP	Activator of kinases	22580	Acros Organics
Cantharidin	Inhibitor of protein phosphatase 2A (IC_{50}= 40 nM)	210155	EMD Millipore Chemicals
(+)-Catechin	Natural flavonoid with antioxidant, chemopreventative, and antitumor properties	ASB-00003310	ChromaDex
CDC25 phosphatase inhibitor I	Inhibitor of CDC25 phosphatase family (IC_{50} = 2.4, 3.9, 6.3, 5.4, and 4.6 μM for 25A, 25B2, 25B3, 25C, and 25C-cat, respectively)	217691	EMD Millipore Chemicals
CDK2 inhibitor II	Inhibitor of CDK2 (IC_{50} = 60 nM)	219445	EMD Millipore Chemicals
CDK4 Inhibitor II NSC	Inhibitor of CDK4/cyclin D1 (IC_{50} = 200 nM)	219477	EMD Millipore Chemicals

CDK4 Inhibitor III	Inhibitor of CDK4 (IC_{50} = 6.0 μM for CDK4/D1 and > 200 μM for CDK2/A)	219478	EMD Millipore Chemicals
CDK4/6 inhibitor IV	Inhibitor of CDK4 and CDK6 (IC_{50} = 1.5 and 5.6 μM, respectively)	219492	EMD Millipore Chemicals
Cerulenin	Antifungal, inhibitor of FAS	ICN19509801	MP Biomedicals
Citric acid monohydrate	Phosphofructokinase inhibitor, glycolysis regulator	12491	Acros Organics
Curcumin	Anti-inflammatory, inhibitor of LO	21858	Acros Organics
Cycloheximide	Antiobiotic, inhibitor of protein synthesis	35742	Acros Organics
D-Glucosamine hydrochloride	Component of chitosan, used to treat osteoarthritis	11990	Acros Organics
Eicosapentaenoic acid	Fatty acid, inhibitor of COX	NC9297605	Cell Signaling Technology
(-)-Epicatechin	Antioxidant, natural product from green tea	ASB-00005125	ChromaDex
(-)-Epicatechin gallate	Antioxidant, natural product from green tea, inhibitor of protease (FAB1 inhibitor, IC_{50} = 0.2 μM)	ASB-00005135	ChromaDex
(-)-Epigallocatechin	Antioxidant, natural product from green tea	ASB-00005145	ChromaDex
(-)-Epigallocatechin gallate	Polyphenol catechin antioxidant found in green tea, antitumor, antioxidant, anticarcinogenic, antimutagenic, anti-inflammatory, and neuroprotective activity, inhibitor of iNOS (NOS II), MAP kinase mediated signalling pathways, telomerase and DNA methyltransferase, and FABI (IC_{50} = 0.2 μM)	ALX-270263	Axxora (or ChromaDex)
D,L-Epinephrine	Hormone, inhibitor of adrenergic receptors	2151064	MP Biomedicals
Erbstatin analog	Inhibitor of the EGFR associated tyrosine kinase1 and histone lysine methyltransferase G9a (IC_{50} = 2.818 μM)	2158813	MP Biomedicals
Esculetin	Inhibitor of LO and activator of MAPK	E0386	TCI America
ET-18-OCH3	Cytotoxic agent that shows selective cytocidal activity against neoplastic cells and virally transformed cells, inhibitor of phosphatidylinositol-specific phospholipase C (PI-PLC, IC_{50} = 9.6 μM)	341207	EMD Millipore Chemicals
Ethyl 3,4-dephostatin	Inhibitor of PTP1b (IC_{50} = 3.2 μM)	263203	EMD Millipore Chemicals
Ethyl palmitate	Fatty acid, anti-inflammatory activity	--[b]	Acros Organics
FAAH Inhibitor I	Inhibior of fatty acid amide hydrolase (IC_{50} = 396 nM)	341248	EMD Millipore Chemicals
FAAH Inhibitor II	Inhibitor of fatty acid amide hydrolase (IC_{50}= 4.6 nM)	341249	EMD Millipore Chemicals
Forskolin	Inhibitor of MAPK, stimulates cAMP, activator of PKA, activator of adenylate cyclase	BP25201	Fisher BioReagents (or AK Scientific)
Genistein	Isoflavone, antioxidant, inhibitor of tyrosine kinase, inhibior of PPAR, inhibitor of topoisomerase	32827	Acros Organics
Gibberellic acid	Plant hormone, stimulates seed germination	41091	Acros Organics
Glycerol	Triacylglycerol precursor	BP229	Fisher BioReagents
Gossypol	Plant phenol, inhibitor of PKC	195210	MP Biomedicals
Halopemide	Antagonist of dopamine receptor, inhibitor of phospholipase D2	H3041	Sigma Aldrich

Ibuprofen	Inhibitor of COX	25861	Acros Organics
Indole acetic acid (IAA)	Auxin plant hormone	12216	Acros Organics
Indole-3-butyric acid	Plant growth hormone	ICN10204 301	MP Biomedicals
Indomethacin	Inhibitor of COX	A19910	Alfa Aesar
Jasmonic acid	Plant growth regulator	50213381	Research Products International
JZL184 hydrate	Inhibitor of monoacylglycerol lipase (IC_{50}= 6 nM)	J3455	Sigma Aldrich
K-252a	Inhibitor of PKC (Ki = 25 nM), trk tyrosine kinase family members (gp140trk, IC_{50} = 3 nM) and cGMP-dependent protein kinase	BML-EI152	Enzo Life Sciences
Kenpaullone	Inhibitor of CDK1/cyclin B (IC_{50}= 400nM), CDK2/cyclin A (IC50 = 680nM), CDK5 (IC_{50}= 850nM), GSK-3 β inhibitor (IC_{50}= 23 nM).	BML-EI310	Enzo Life Sciences
Ketoconazole	Inhibitor of cytochrome P450 (progesterone 15-alpha hydroxylase, IC_{50}= 0.369 nM) and 14-alpha-demethylase, antifungal agent (IC_{50}= 0.01 μM) against *Trichophyton rubrum*	BP2734	Fisher BioReagents
Kinetin	Plant growth regulator, activator of cAMP, inhibitor of Rho kinase 2	22650	Acros Organics
Lactic acid	Intermediate in the fermentation of sugar	BP26615	Fisher BioReagents
SB202190	Inhibitor of p38 MAPK (p38 α and β isoforms, IC_{50}= 50 and 100 nM at SAPK2a/p38 and SAPK2b/p38 β 2, respectively)	50-810-911	Tocris Cookson
Methyl jasmonate	Plant hormone and defense compound	M1068	TCI America
Naproxen	Inhibitor of COX	2190247	MP Biomedicals
Naphthyl acid phosphate, monosodium salt	Broad-spectrum inhibitor of PTP	479775	EMD Millipore Chemicals
Olomoucine	Inhibitor of CDC2 protein kinase (IC_{50}= 6 μM), CDK1 (IC_{50}= 4.6 μM), and CDK2 (IC_{50}= 7 μM)	V2372	Promega
Orlistat (tetrahydrolipstatin)	Diacylglycerol lipase inhibitor (IC_{50}= 1 μM)	O4139	Sigma Aldrich
PD98059	Inhibitor of cytochrome 9450, MEK1 activation and the MAPK cascade	9900	Cell Signaling Technology
Phorbol 12-myristate 13-acetate	Inhibitor of PKC	P-1680	LC Laboratories
Piceatannol	Plant metabolite, inhibitor of PKA (rat liver catalytic subunit; IC_{50}= 3 μM), PKC (IC_{50}= 8 μM), and MLCK (IC_{50}= 12 μM)	527948	EMD Millipore Chemicals
PP2	Inhibitor of Src family of protein tyrosine kinases. Inhibits p56lck p59fynT & Hck	529573	Andwin Scientific
Propyl gallate	Antioxidant, inhibitor of microsomal lipid peroxidation (IC_{50} = 4.5 μM)	13158	Acros Organics
Palmityl trifluoromethyl ketone	Inhibitor of calcium-dependent phospholipase A2 (IC_{50} = 3.8 μM)	P8727	Sigma-Aldrich
PTP Inhibitor II	Inhibitor of PTP (K_i = 128 μM)	540205	EMD Millipore Chemicals
Quinacrine	Inhibitor of PLA2 and MAO	551850	EMD Millipore Chemicals
Rapamycin	Immunosuppressant, blocks signaling that leads to p70 S6 kinase activation (IC_{50}= 50 pM)	R-5000	LC Laboratories

Resveratrol	Phenolic with antifungal, antitumor, and antioxidative properties. Inhibitor of COX-1 (ED_{50} = 15 μM)	554325	EMD Millipore Chemicals
RHC 80267	Diacylglycerol lipase inhibitor, important second messenger in signal transduction pathways	R2028	Sigma Aldrich
Roscovitine	Inhibitor of CDKs (p34cdk1/cyclin B, IC_{50}= 650 nM)	557360	EMD Millipore Chemicals
Salicylic acid	Anti-infective, antifungal, and keratolytic agent, inhibitor of human carbonic anhydrase 2 (K_i = 7.1 μM)	41922	Acros Organics
Staurosporine	Indolocarbazole, inhibitor of PKC which enhances cAMP-mediated responses, inhibitor of the ERK signaling pathway (EGFR, IC_{50}= 0.4467 μM)	BP2541100	Fisher BioReagents
SU9516	Inhibitor of CDKs (IC_{50}= 22 nM)	572650	EMD Millipore Chemicals
Vitamin E	Plant tocopherol, antioxidant	--[b]	Alfa Aesar
Theobromine	Plant alkaloid, inhibitor of ERK signaling pathyway (potency = 0.004 μM)	25882	Acros Organics
Zeatin	Cytokinin, plant growth regulator	26429	Acros Organics

[a] When readily available, biological activity is listed based on information obtained from vendor website, PubChem, or Wikipedia. [b] Item is no longer available from vendor. Abbreviations are as follows: EGFR = epidermal growth factor receptor, CDK = cyclin dependant kinase, ERK = extracellular signal regulated kinase, GSK = glycogen synthase kinase, MAPK = mitogen-activated protein kinase, PKC = protein kinase C, AMP = adenosine monophosphate, CDC = cell division cycle, PLA = phopholipase A, PTP = protein tyrosine phosphatase, PPAR = peroxisome proliferator-activated receptor, FAS = fatty acid synthesis, FAB = fatty acid biosynthesis, MLCK = myosin light chain kinase, MAO =monoamine oxidase, COX = cyclooxygenase, LO = lipoxygenase, iNOS = inducible nitric oxide synthase, and AMPK = AMP-activated protein kinase.

II. Microplate Assay

Sodium bicarbonate supplementation for assay preparation. Assay plates consisted of 100 μL of microalgae cell suspension in 150 μL of appropriate media that was dispensed using an automated plate dispenser (Microflo Select, Biotek, Vermont, USA). Microalgae were grown in a 96-well microplate (Corning 3370) covered with a clear lid and sealed with parafilm along the edges to minimize evaporation. For *N. salina* and *P. tricornutum*, supplemental sodium bicarbonate (1.2 g/L concentration) was added to media to provide optimal growth conditions, based on our preliminary studies of microalgae growth levels in microplates.

To establish if supplemental carbon was required for optimal growth of each microalgae strain in microplates, growth experiments were first performed for all algae species using a gradient of sodium bicarbonate (2x dilution ranging from 0.3-1.2 g/L) in media, and investigated with and without the addition of 0.4% DMSO (**Fig S1-S4**). From these experiments, it was determined that a concentration of 1.2 g/L sodium bicarbonate produced the optimal growth based on cell density (i.e. absorbance) in both *P. tricornutum* and *N. salina*, thus 1.2 g/L was utilized for microplate assays with these strains. Low concentrations or no addition of sodium bicarbonate was determined to be more optimal for growth of *N. oculata* and *Nannochloris sp.* in microplates, thus no supplemental sodium bicarbonate was utilized for microplate assays with these strains.

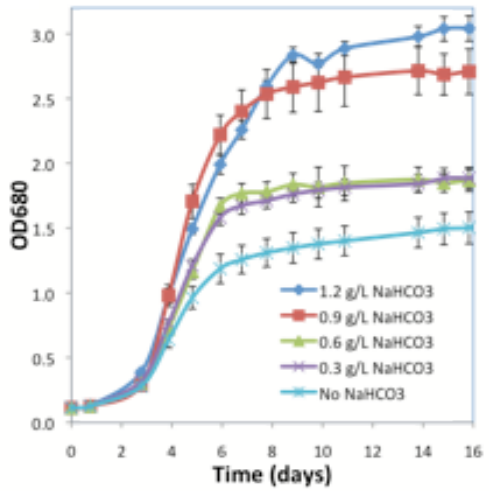

Figure S1. Evaluation of sodium bicarbonate for growth optimization of green microalgae *N. salina* in microplates. Experiments were performed with a dilution concentration gradient of 0.3-1.2 g/L sodium bicarbonate. Growth was monitored daily by measuring absorbance at 680 nm until stationary growth phase. Growth curves were compared between strains grown in F/2 media. Error bars represent the s.e.m. of three replicates.

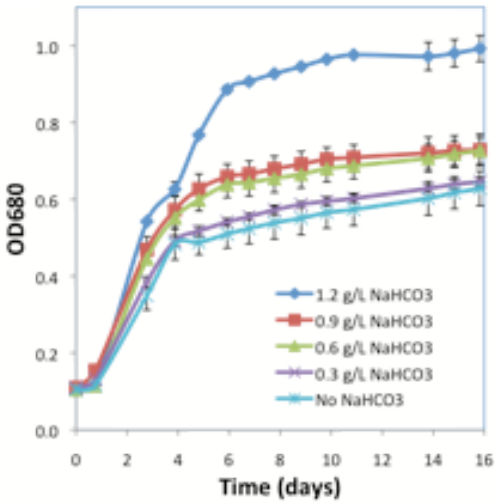

Figure S2. Evaluation of sodium bicarbonate for growth optimization of diatom *P. tricornutum* in microplates. Experiments were performed with a dilution concentration gradient of 0.3-1.2 g/L sodium bicarbonate. Growth was monitored daily by measuring absorbance at 680 nm until stationary growth phase. Growth curves were compared between strains grown in F/2 media. Error bars represent the s.e.m. of three replicates.

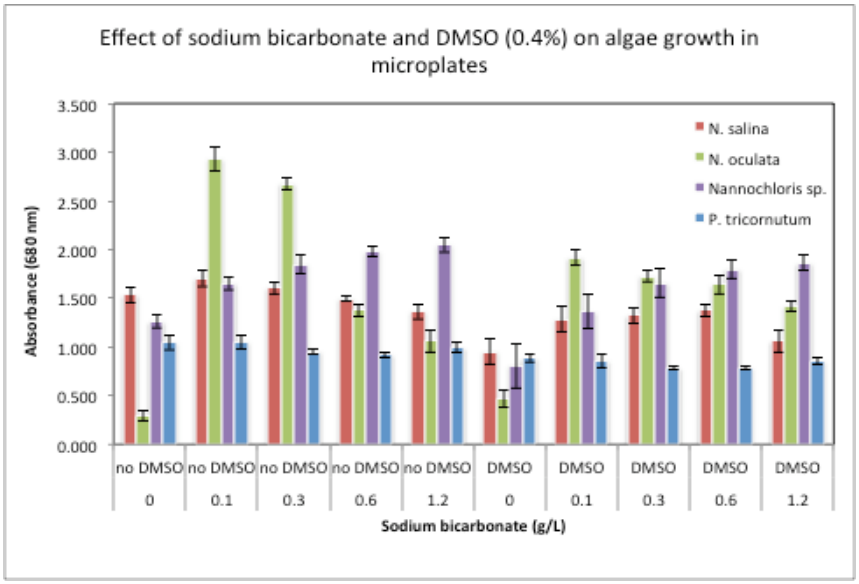

Figure S3. Comparison of the effects of sodium bicarbonate (0.1-1.2 g/L) with DMSO (0.4%) on microalgae growth in microplates. The absorbance unit at late stationary phase (Day 16) were compared with and without DMSO for all four microalgae strains. Growth comparison was based on absorbance value. Error bars represent the standard deviation of six replicates.

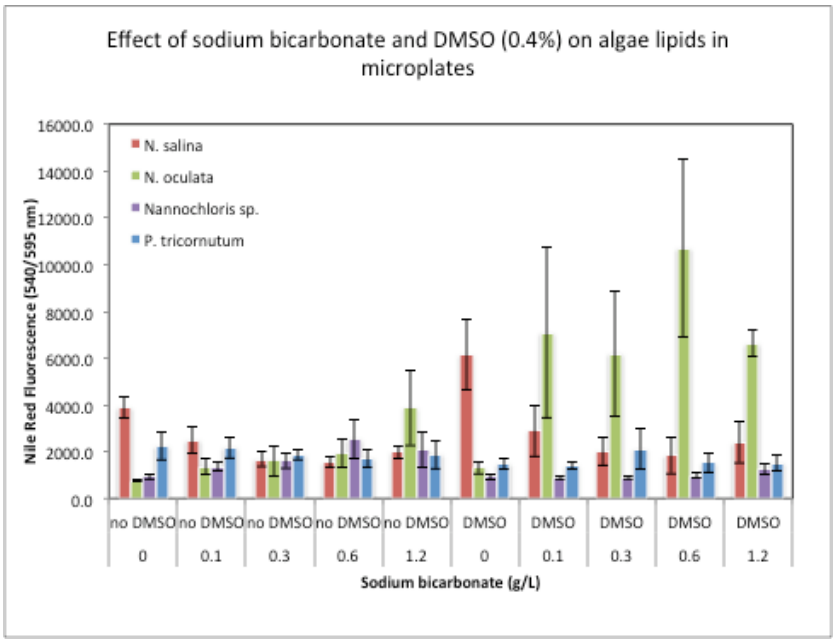

Figure S4. Comparison of the effects of sodium bicarbonate (0.1-1.2 g/L) with DMSO (0.4%) on microalgae lipid production in microplates. Intracellular lipids were compared at late stationary phase (Day 16) with and without DMSO for all four microalgae strains based on the maximum Nile Red fluorescence intensity. Error bars represent the standard deviation of six replicates.

Preparations of compounds and microalgae in microplates. Microplate assays were investigated with either three or four replicates along with a separate microplate containing only control wells to compare growth. Due to extensive evaporation in exterior wells over time due to edge effects, our unique algae plate layout is designed to use the 60 interior wells out of 96 wells

for the experiment. The 36 outer wells are filled with millipore-filtered water and media to prevent evaporation and edge effects in the inner algae wells, as well as serve as blanks. The 60 wells in the center contain a total volume of 251 μL (100 μL of media + 1 μL DMSO compound stock + 150 μL dilute algae stock). All dilutions started from 10 mM compound stock in DMSO. DMSO stock solution is added first to the microplate containing media only so that the exothermic reaction of DMSO and media does not negatively affect algae growth. To each control wells, 1 μL of DMSO was added. Microplates resume the same shaker position after each analysis. Compounds investigated with water delivery (in place of DMSO) were added to microplates before the addition of microalgae.

Microalgae growth conditions in microplates. Microalgae were grown in 96-well clear, round, flat-bottom microplates (Costar 3370). Clear microplates were necessary in order to give maximum light exposure for optimal growth of microalgae during the assay. The plates were grown under full spectrum incident uniform lighting at a 16:8 hour light/dark cycle with 90-150 μM photons/m^2/s (High Efficiency T-5 Grow Lights – Gardeners Supply Co, Vermont). The shakers were kept at a constant orbital shaking of 150 rpm. Ambient temperature is 22 ± 3 ˚C. Absorbance (680 nm) and chlorophyll fluorescence (excitation at 360 nm and emission at 645 nm) analysis were taken every day on the Synergy HT Multi-mode Plate Reader (Biotek, Vermont, USA), in order to monitor cell density and chlorophyll production in algae over the growth cycle.

Nile Red Optimization: Method A (original optimization) and B (final optimization) for intracellular lipid screening and analysis in microplates. Intracellular lipid levels were directly analyzed for microalgae grown in clear microplates using an optimized Nile Red protocol at approximately 2-3 days at stationary phase (to allow for lipid accumulation). A related Nile red procedure has been reported for analysis of whole cell microalgae suspension from a concentrated microalgae pellet.[1] Optimization experiments were performed relying on the correlation of intracellular lipids with the quantity of cells, based on cell density measurements.

For diatom, *P. tricornutum*, the addition of 25 μL of 1 mg/mL Nile Red dye dissolved in acetone with fluorescent emission analyzed at room temperature (~22˚C) was found to effectively measure lipid changes in microplates (**Fig S5**). Green microalgae required additional optimization involving the addition of DMSO and heat to allow Nile Red to penetrate through the thick cell exterior. The original optimized method involved the addition of 25 μL of 1:1 (v/v) DMSO:media added manually using a multichannel pipette and the microplate was vortexed with an IKA® MS 3 Digital plate shaker for one minute. Then, 25 μL of Nile Red dye (1 mg/mL solution in acetone) was added manually to the microplate using a multichannel pipette. Immediately after Nile Red dye was added to all wells, the microplate was vortexed for ~30 s and inserted into the Biotek Synergy HT Multi-mode platereader, which had been preheated to 40˚C. The microplate was allowed to sit inside the instrument avoiding ambient light for ten minutes of staining time before analysis. Then fluorescence data was acquired at 40 ˚C using a 20-min kinetic read with continuous shaking at intervals of 52 s, automatically set by the instrument. Fluorescence was acquired with an excitation and emission wavelength of 530 and 590 nm, respectively. Fluorescence data selected for analysis/comparison is based on the maximum intensity from the kinetic read.

A modified procedure was developed for a more rapid lipid analysis by omitting the 10-minute staining time, reducing heating temperature to 35 ˚C, and using automated dispensing of Nile Red dye. Nile Red fluorescence data is acquired immediately after dispensing Nile Red

using a plate dispenser (Biotek Microflo Select), which minimizes dispensing time and gives a more even dye exposure.

Our Nile Red protocol for microplates was optimized to measure total intracellular lipid in diatom *P. tricorntum* and green microalgae *N. salina, N. oculata*, and *Nannochloris sp*. For initial Nile Red optimization studies, we use a dilution series of microalgae where an increase in cell density will correlate with an increase in the level of intracellular lipids. The amount of cells plated were verified using absorbance and chlorophyll fluorescence to show an increasing percentage of microalgal suspension in media (**Fig S5A and S5D**). With optimized conditions, the maximum Nile Red fluorescence intensity demonstrates a comparable increase with increasing microalgal cells, indicating that our conditions are effective to allow Nile Red to enter the cell to stain intracellular lipids (**Fig S5B and S5E**). Due to thicker cell walls and variation for green microalgae strains, thus heat and chemical addition is necessary to allow the uptake of the dye into the cell.[1] The fluorescent signal of Nile Red has been reported to differ between species and accounts for the difference observed in the emission curves between green microalgae and diatoms.[2] We observe an increase in Nile Red fluorescence intensity in a stepwise fashion when cell concentration increases (total neutral lipids) as shown in **Figures S5C and S5F**. Nile Red fluorescence analysis is shown as a 30 minute kinetic analysis, but 20 minutes is also adequate to observe the maximum fluorescence intensity. Other lipophilic dyes[3] and assays for lipid detection were also investigated, but proved more difficult to adapt to a whole-cell high-throughput microplate format. We analyzed the fluorescence emission for all strains and compounds and consistently observed that the maximum fluorescence emission intensity appears within the time range of 20 minutes, therefore 20 minutes was chosen for all of our analysis and variation in data is minimized.

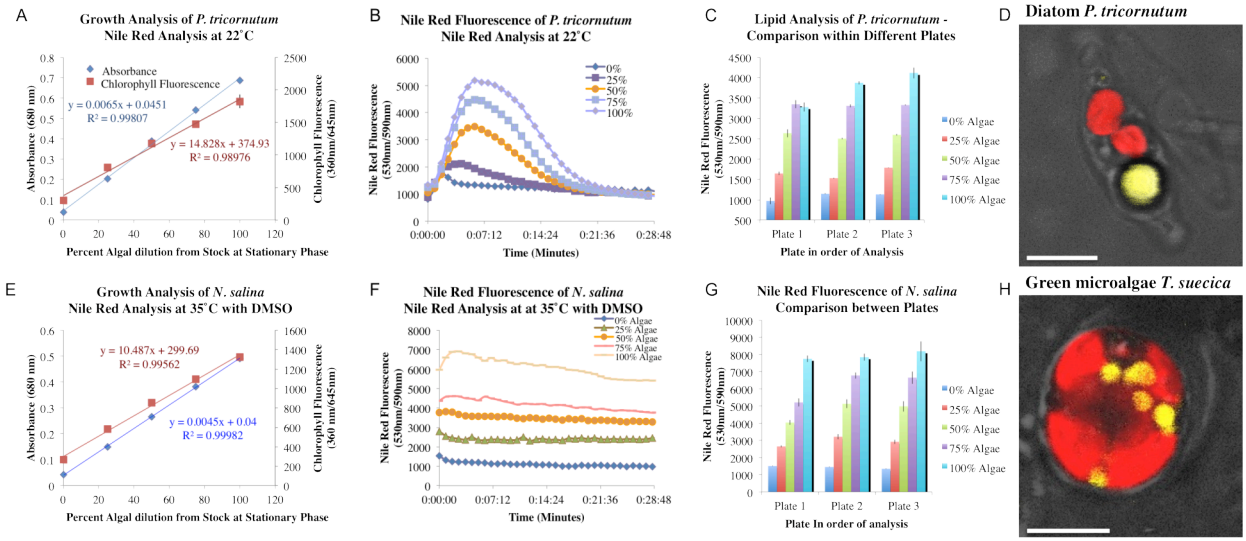

Figure S5. Nile Red optimization for measuing intracellular lipids with diatom *P. tricornutum* and green microalgae *N. salina*. Cell density verification for *P. tricornutum* (A-D) and *N. salina* (E-G) were measured using absorbance at 680 nm and chlorophyll fluorescence at excitation and emission wavelength of 360nm/645nm. Total volume of microalgae suspension in media is 250 μL per well. Nile Red protocol for *P. tricornutum* is the addition of 25 μL 1 mg/mL of Nile Red dye dissolved in acetone before Nile Red fluorescence analysis for 30 minutes at excitation and emission wavelength at 530 nm and 590 nm, respectively. As for *N. salina*, the addition of 25 μL of 1:1 v/v DMSO:F/2 media was dispensed to each well before the addition of Nile Red. Fluorescence analysis was investigated at 35˚C. Kinetic analysis of Nile Red fluorescence intensity for *P. tricornutum* (B) and *N. salina* (F) over the course of 30 minutes in one well. Six wells were averaged per algae concentration per plate (C and G). Images of Nile Red staining intracellular lipids in diatom *P. tricornutum* (D) and representative green microalgae *T. suecica* (H) cells where red indicates chlorophyll autofluorescence and yellow indicates Nile Red fluorescence.

Fluorescent images were acquired using an Olympus FV1000 laser scanning confocal microscope using an DM488/543/633 excitation filter at bandpass filter centered at 572 nm with range of 38. Chlorophyll autofluorescence and transmitted light were simultaneously obtained using a 633-nm and 488-nm laser, respectively. All scale bars represent 5 μm. Argon 488-nm laser were utilized for Nile Red fluorescence with bandpass filter Error bars represented in absorbance (A and D), chlorophyll fluorescence (B and F) and nile red fluorescence (C and G) are based on the standard deviation of six well replicates per microalgae concentration. The error bars in absorbance and chlorophyll are not visible because the standard deviation is approximately 0.01.

Control experiments investigating effect of compounds to enhance or quench chlorophyll and/or Nile Red fluorescence. We performed control experiments to analyze chlorophyll and neutral lipid content of microalgae immediately after the addition of compounds at 40 μM (the highest screening concentration) to investigate whether compounds contribute to quenching or enhancing chlorophyll and/or Nile Red fluorescence. (Separate experiments were performed to confirm that none of the screening compounds exhibited autofluorescence.) These control experiments were performed with in *N. oculata* and *P. tricornutum* as representative micoalgae strains. The 54 compounds investigated in our initial screen were added to the center wells in a 96-well microplate at 40 μM concentration. Microalgae were dispensed to all wells in a 96-well microplate from the same stock. Chlorophyll fluorescence was analyzed by measuring fluorescence at excitation wavelength of 360nm and emission wavelength of 645nm. Neutral lipids were measured following the Nile Red protocol that we optimized for green microalgae. An example of results with *N. oculata* is shown in Figure S6.

It was observed that two compounds out of 54 (PD98059 and atrazine) showed effects at 40 μM that indicate potential enhancement of chlorophyll fluorescence in *N. oculata*. PD98059 was not identified as an active compound in the screening at 40 μM or any other concentration. Atrazine was identified as a compound with some activity, with an optimal concentration at 4 nM, where no enhancement of chlorophyll fluorescence was observed. Four compounds out of 54 (quercetin, SU-9516, baicalein, and apigenin) showed effects that indicate potential quenching of chlorophyll fluorescence in *N. oculata*. Except for PD98059, compounds did not have a major affect on chlorophyll fluorescence in *P. tricornutum*. There was no effect of compounds on Nile Red fluorescence intensity that was more significant than the inherent variation of cell density due to the liquid dispenser. Compounds utilized in the initial screening assay show similar Nile Red fluorescence intensities compared to microalgae with DMSO, the solvent used to dissolve compounds. These control experiments confirm that compounds used in our initial screening assay do not enhance or quench Nile Red fluorescence at 40 μM. Additional confirmation of compound activity is also provided based on dose-response screening, where the lower concentrations are used.

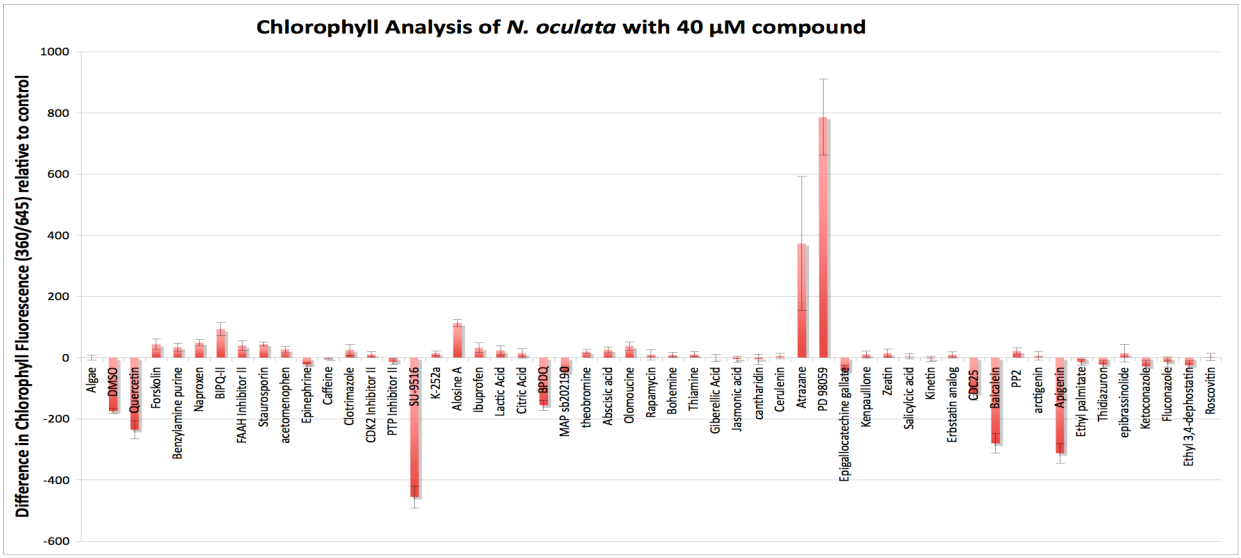

Figure S6. The effect of 40 μM compound treatment on chlorophyll fluorescence of *N. oculata*. Chlorophyll fluorescence was analyzed by measuring fluorescence at excitation wavelength of 360nm and emission wavelength of 645nm. The graph shows the difference in fluorescence intensity relative to no-compound treatement. Error bars represent standard error of three replicates, one replicate per 96-well microplate.

Statistical analysis and summary of positive hits identified in microplate screening.

A comparison between data for control vs. compound-treated microalgae was employed to evaluate the effect of each compound on lipid production, based on Nile Red fluorescence intensity with measurements performed at excitation and emission wavelength at 530 nm and 590 nm, respectively. A compound was selected as a "hit" when the result is statistically significant at a p-value < 0.05. P-values were calculated based on independent or unpaired analysis using a two-tailed test with unequal variance for the Nile Red fluorescence intensity using the t-test. Microalgae were screened with 54 different compounds per plate with three separate plate replicates analyzed simultaneously ($n = 3$). Control wells containing microalgae treated with vehicle only (i.e. DMSO) were grown within the same plate, as well as in a separate microplate containing only control wells. The minimum number of control wells for all data analyzed was 18. The first arrays consisted of all the control values investigated and the second array consisted of the desired compound with three replicates. A high number of hits were also observed with p-values less than 1%. Although the hit could be the result of compounds producing a negative or positive effect relative to the control, here only the compounds that show increases in lipid production are listed. Refer to **Table S3** for a summary of compound names.

Table S2. Number of compounds identified with positive effects in microplate screening with p-values < 0.05 and < 0.01.

Algae species	Concentration	Total number of hits ($p < 0.05$)	Number of hits with increase relative to control ($p < 0.05$)	Total number of hits ($p < 0.01$)	Number of hits with increase relative to control ($p < 0.01$)
P. tricornutum	40 μM	22	2	21	2
	200 nM	11	3	9	2
Nannochloris sp.	20 μM	8	0	7	0
	200 nM	11	10	1	0
N. salina	20 μM	17	11	12	6
	200 nM	2	0	1	0
N. oculata	20 μM	26	24	18	17
	200 nM	11	10	6	5

Microalgae were screened with three plate replicates analyzed simultaneously (n = 3). The maximum Nile Red fluorescence intensities of each well were used for calculating p-values using an independent, two-tailed t-test with unequal variance in Microsoft Office Excel. Refer to **Table S3** for a summary of compound names.

Table S3. A summary of compounds indicate a positive effect (>20% increase) for intracellular lipid levels based on Nile Red fluorescence intensity in the initial microplate screening

Algae	Molecule	Nile Red Fluorescence % Increase	P value
P. tricornutum (compounds tested at 40 μM)	CDK2 inhibitor II	150.6	9.56E-11
	SB 202190	115.0	7.04E-03
P. tricornutum (compounds tested at 200 nM)	Benzylaminopurine	105.9	4.67E-02
	CDK2 inhibitor II	50.3	1.53E-05
	Kinetin	25.2	4.47E-03
	Abscisic acid	87.0	1.96E-05
N. oculata (compounds tested at 200 nM)	Epigallocatechin gallate	207.5	4.52E-02
	Zeatin	157.1	3.23E-02
	Arctigenin	152.2	4.91E-02
	AG82	144.5	2.14E-02
	Rapamycin	141.6	2.25E-02
	Cycloheximide	137.9	4.88E-02
	Epinephrine	129.3	1.96E-02
	Lactic Acid	128.8	3.74E-02
	Resveratrol	120.4	4.43E-02
	Aloisine A	117.7	3.67E-02
N. salina (compounds tested at 20 μM)	PTP Inhibitor II	87.2	4.57E-02
	Bohemine	61.0	1.50E-02
	Ibuprofen	59.0	5.07E-08
	Baicalein	37.3	6.46E-03
	Kenpaullone	34.8	1.05E-11
	Abscisic acid	34.5	3.96E-03
	Apigenin	34.3	3.64E-02
	Ketoconazole	32.0	3.31E-02
	Salicylic acid	25.5	1.83E-06

Nannochloris sp. (compounds tested at 20 μM)	Epigallocatechin gallate	214.9	2.18E-02
	Apigenin	136.7	9.14E-05
	CDC25	130.9	5.21E-10
	Bohemine	122.0	1.68E-02
	Rapamycin	117.3	3.13E-04
	Kenpaullone	97.7	3.25E-02
	Indole acetic acid	95.4	1.24E-03
	Acetaminophen	89.7	2.11E-04
	Ibuprofen	80.2	5.35E-11
	SB 202190	54.6	2.32E-02
	AG82	54.2	5.56E-03
	Resveratrol	53.3	1.28E-03
	Forskolin	45.3	7.33E-03
	Epinephrine	44.9	7.79E-10
	Erbstatin analog	40.5	2.42E-03
	Salicylic acid	32.3	1.92E-03
	Lactic Acid	30.9	3.68E-02
	Roscovitine	30.8	3.46E-04
	SB 202190	28.8	1.55E-02
	PTP Inhibitor II	27.8	2.96E-02
	Cantharidin	22.9	8.39E-05
Nannochloris sp. (compounds tested at 200 nM)	Ketoconazole	258.9	7.13E-05
	Bohemine	146.3	2.06E-02
	Cerulenin	107.9	8.07E-04
	Abscisic acid	90.8	3.42E-02
	Kenpaulllone	84.2	2.54E-02
	Jasmonic acid	80.5	3.07E-02
	Erbstatin analog	80.2	2.92E-12
	Salicylic acid	37.0	3.16E-02
	Theobromine	34.3	8.83E-03
	CDC25	28.2	4.02E-05

Compounds listed show an increase in Nile Red fluorescence intensity compared to the control. The initial screening involves a microplate assay with six controls in each plate for four different microalgae strains. A separate control plate consist of 54 control wells with DMSO to factor in controls in different wells in the plate. The assay was investigated at two concentrations per algae strain, three replicates per compound, one compound per plate. Nile Red fluorescence was analyzed utilizing Nile Red method A described above. Compounds listed show an increase in intracellular lipid levels and are all statistically significant ($p < 0.05$).

III. Dose-response Screening in Microplates

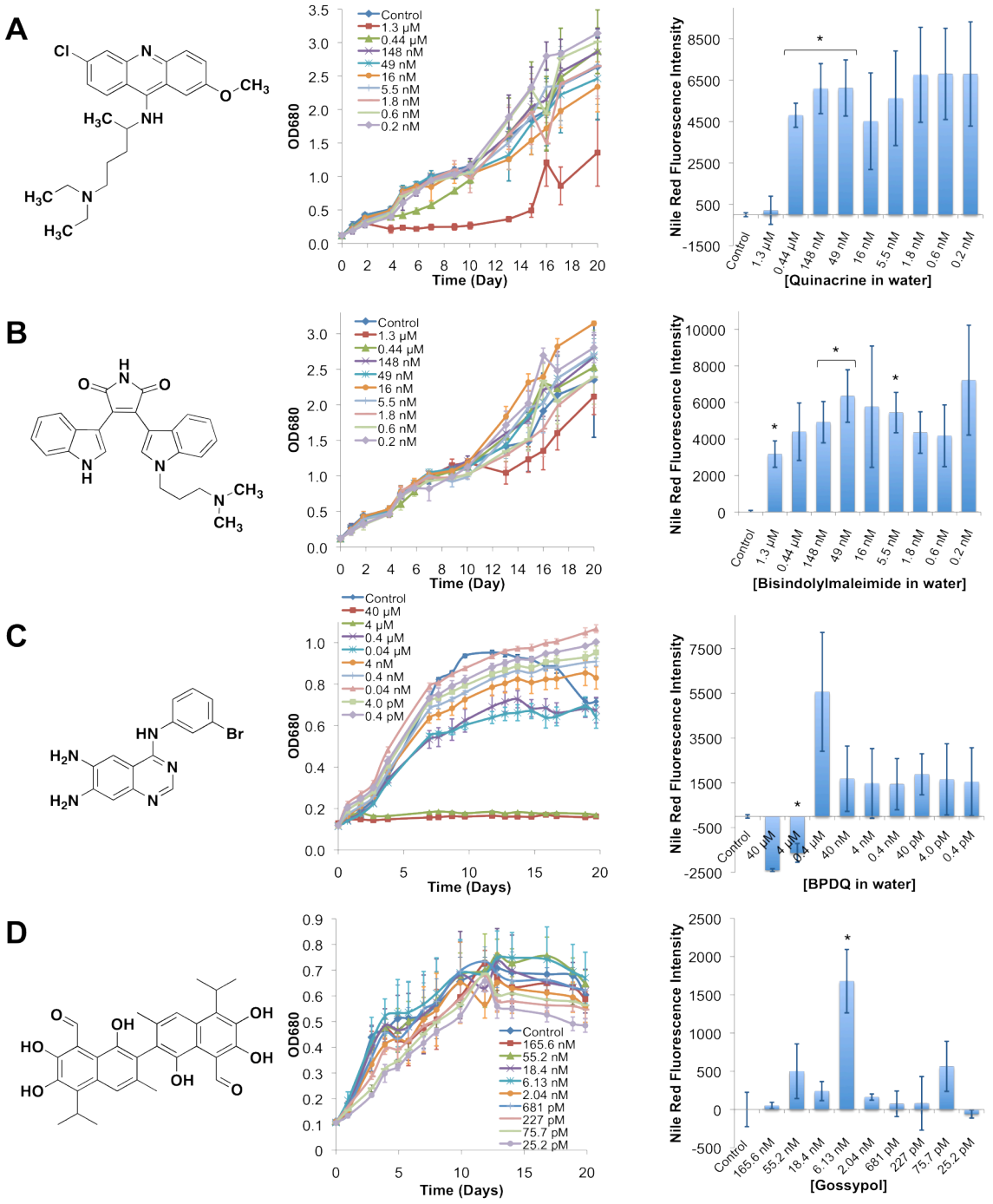

Figure S7. Dose-response effects for growth rate and intracellular lipid levels in microalgae. A) Dose-response effects of quinacrine delivered in water with *Nannochloris sp*. B) Dose-response effects of bisindolylmaleimide delivered in water with *Nannochloris sp*. C) Dose-response effects of BPDQ in water with *N. salina*. D) Dose-response effects of gossypol with *N. salina*. Cell density was measured by optical density at 680 nm. Nile Red fluorescence (530/590 nm) intensity values represent the difference relative to the control measured. Data points and error bars (s.e.m.) in optical density and Nile Red fluorescence measurements represent the mean of three replicates. * denotes concentrations that are statistically significant ($P < 0.05$, two-tailed *t*-test).

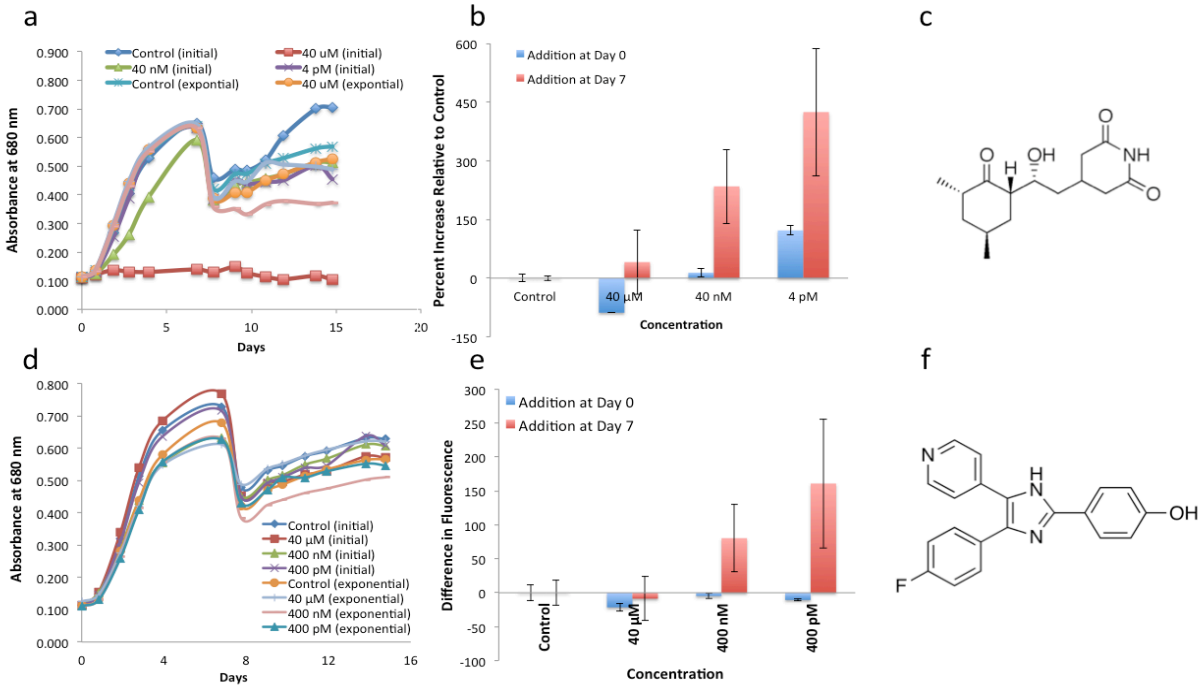

Figure S8. Examples of temporal effects for cycloheximide and SB202190 screened in *P. tricornutum*. (a) Comparing growth analysis with the addition of cycloheximide in the initial phase (day 0) and at exponential phase (day 6). (b) Comparing lipid analysis based on Nile Red fluorescence intensity at harvest (day 16) showing temporal effects for cycloheximide on intracellular lipid levels. c) Molecular structure of cycloheximide. (d) Comparing growth analysis with the addition of SB202190 in the initial phase (day 0) and at exponential phase (day 6). (e) Lipid analysis based on Nile Red fluorescence intensity were compared at harvest (day 16) showing temporal effects for SB202190 on intracellular lipid levels. (f) Molecular structure of SB202190. Error bars represent s.e.m. for the difference in absorbance (a and d) and Nile Red fluorescence (b and e) represent the standard deviation of 3 replicates. The error bars in absorbance measurements are not visible because the standard deviation for each data point is approximately 0.01.

Table S4. Compounds from the dose-response microplate screening that exhibit Nile Red fluorescence increases approximately ≥50% ($p < 0.05$)

Microalgae Strain	Compound	Concentration	% Increase based on Nile Red Fluorescence Intensity
N. oculata	Quinacrine[a]	244 pM	106
	Quinacrine[a]	61 pM	100
	Sb202190[d]	400 fM	95
	Quinacrine[a]	976 pM	93
	Baicalein (water)***	40 μM	76
	Quinacrine[a]	4 nM	75
	Quinacrine*[a]	15.6 nM	66
	Baicalein	25.2 pM	52
	Curcumin	75.7 pM	49
N. salina	Epigallocatechin gallate*[c]	1.48 μM	217
	Epigallocatechin gallate**[c]	4.44 μM	214
	Epigallocatechin gallate[c]	13.3 μM	136
	BPDQ	6.0 nM	130
	JZL 184 hydrate[b]	40 μM	119
	Gossypol	6.13 nM	103
	Epigallocatechin gallate[c]	493 nM	87
	BPDQ	55 nM	86
	Methyl jasmonate	13 nM	85
	BPDQ	494 nM	73
	Forskolin	4.6 nM	66
	Zeatin***	4.6 nM	64
	Arctigenin**	370.4 nM	64
	BPDQ	6.10 nM	63
	Arctigenin*	4.6 nM	63
	Esculetin	6.13 nM	62
	Indomethacin	123.5 nM	61
	Arctigenin	13 nM	59
	PTP Inhibitor II	227 pM	54
	Atrazine	4.6 nM	53
	Zeatin	13 nM	50
	Esculetin	681 pM	50
	CDK4 inhibitor 1	40 μM	49
	Kinetin*	4.6 nM	48
Nannochloris sp.	FAAH inhibitor I (water)	0.6 nM	189
	FAAH inhibitor I (water)	5.5 nM	188
	FAAH inhibitor I (water)	1.8 nM	187
	FAAH inhibitor II (water)	0.6 nM	182
	FAAH inhibitor II (water)	148 nM	167
	FAAH inhibitor I (water)	440 nM	161
	FAAH inhibitor I (water)	49 nM	160
	FAAH inhibitor II (water)	49 nM	154
	FAAH inhibitor I (water)	1.3 μM	152
	FAAH inhibitor II (water)	0.2 nM	145

	FAAH inhibitor II (water)	1.3 μM	144
	Bisindolylmaleimide (water)	49 nM	141
	Quinacrine (water)	49 nM	136
	Quinacrine (water)	49 nM	136
	Quinacrine (water)	148 nM	135
	Quinacrine (water)	148 nM	135
	Bisindolylmaleimide (water)	5.5 nM	121
	Bisindolylmaleimide (water)	148 nM	109
	Quinacrine (water)	440 nM	106
	Quinacrine (water)	440 nM	106
	Indomethacin (water)	5.5 nM	95
	Ketoconazole (water)	148 nM	94
	Indomethacin (water)	49 nM	81
	Piceatannol	6.1 nM	71
	Bisindolylmaleimide (water)	1.3 μM	70
	Cycloheximide[d]	400 nM	408
	CDK2 inhibitor 2	40 μM	347
	Zeatin	4.6 nM	114
	Caffeic acid (water)	4 μM	94
	CDK2 inhibitor 2***	10 μM	86
P. tricornutum	cAMP	370.4 nM	66
	BPDQ (water)	400 fM	63
	Resveratrol	10 nM	61
	Arctigenin	41.2 nM	61
	Naphthyl acid phosphate (water)	681 pM	51
	CDK4/6 inhibitor 4***	10 μM	50

Increases in Nile Red fluorescence intensity were based on three replicates with $p \leq 0.05$ and were analyzed in three different 96-well microplates with the exception of the few compounds. P-values were calculated utilizing a two-tailed test. A lower p-value cutoff was observed for compounds noted by * exhibiting $p < 0.001$, ** $p < 0.0001$, and *** $p < 0.00001$. Compounds with water listed in parenthesis indicate that the compound was dissolved in water for delivery, instead of DMSO. All compounds were added initially (t = day 0). a) Analysis of four replicates within the same plate. b) Analysis of four replicates within different plates. c) Analysis of six replicates within the same plates. d) Compounds were added during exponential phase, at approximately eight days.

IV. Batch Culture experiments

Batch Culture Experiments (500 mL). Microplate well experiments were scaled up to 500-mL batch cultures as the to validate compound efficacy. Batch cultures were grown in 500-mL Corning Pyrex media bottles (Corning 1395-500) using stirring (IKA) with air bubbling (Petco Air Pump). Incoming air was sterile filtered by Polyvent 4 disposable filters (Whatman, Kent, UK). The culture suspensions were maintained with continuous air sparing, continuous elliptical mixing at 100–110 rpm, temperature was maintained at 23 ± 2 °C, and full spectrum incident uniform lighting (High Efficiency T-5 Grow Lights – Gardeners Supply Co, VT) at a 16:8 hour

light/dark cycle with 60-120 M photons/m^2/s. To minimize bacterial contamination, all equipment and materials were autoclaved and media was added to flask in a Labconco Purifier Vertical Clean bench (Labconco, Kansas City, MO). Batch cultures began with microalgae cultures diluted to 0.075 absorbance unit. The amount of DMSO is standardized for all experiments to 0.4%, analogous to microplate experiments, which was selected after investigating the effect of adding various DMSO amounts ranging from 0.04-1.0% on lipid production for batch culture experiments. All 500-mL batch culture contain 2 mL of compound stock solution diluted in DMSO at the desired concentration. Similar to microplates, compounds were added to media before the addition of microalgae. Control cultures are grown without DMSO and compared to cultures grown with 0.4% DMSO. Cell density was measured every other day using a cuvette (1-mL volume) using a Thermo Scientific Genesys 10S Vis Spectrophotometer (ThermoFisher, San Jose) at absorbance of 680 nm.

Lipid extraction and sample preparation from batch cultures. Cells were pelleted by centrifugation at 6000 x *g* at 4°C for 20 minutes (Thermo Scientific RC-6 Plus, rotor SLA-3000, Waltham, MA, USA), washed with Millipore-filtered water, re-pelleted and then lyophilized (Labconco Freezone 6, Kansas City, MO) to dryness (2-3 days). Nonpolar lipids were extracted by sonication (Fisher Scientific Model 120 Sonic Dismembrator, ThermoFisher, San Jose) for 1 min in chloroform, followed by chloroform-methanol extractions, washed with PBS buffer, and dried under vacuum for 12 h (Table S5).[4-9]

Specific Growth Rate Determination. Specific growth rates were calculated for compounds grown in 500-mL cultures using the equation below, where m_{t2} is the absorbance at time 2 (t_2) and m_{t1} is the absorbance at time 1 (t_1) in the most linear section during exponential growth phase. A sample growth curve is shown in Figure S9.[10] Biomass was determined by measuring absorbance at 2-day intervals.

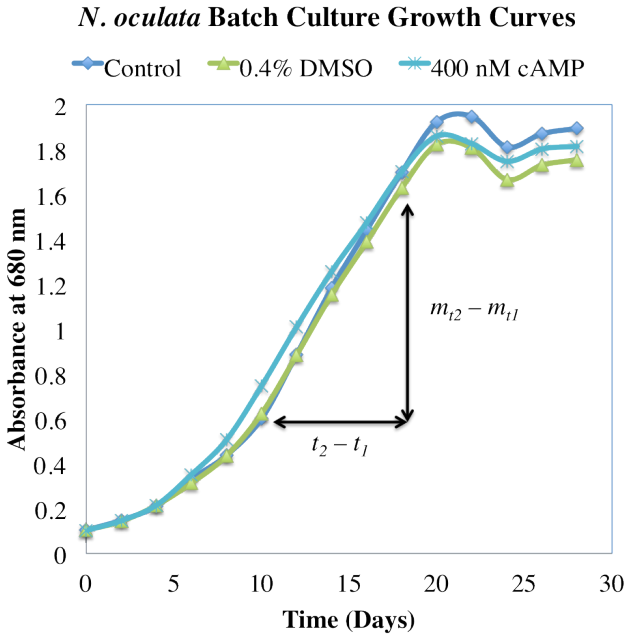

$$\mu = \frac{\ln(m_{t2} - m_{t1})}{t_2 - t_1}, t_2 > t_1$$

Figure S9. Sample growth curve for determining specific growth rate.

Table S5. Chemical triggers for lipid increase in microalgae (500 mL cultures)[a]

Microalgae strain	Compound	Final cell density (680 nm)	Biomass (mg)[b]	Lipid weight (mg)
Nannochloris sp.	Control	1.87 ± 0.37	1185.7 ± 593.5	44.2 ± 13.9
	DMSO (0.4%)	1.82 ± 0.59	772.3 ± 314.3	37.1 ± 2.7
	10 μM Forskolin	2.10 ± 0.16	435.4 ± 384.8	66.9 ± 26.7
	400 nM cAMP	1.81 ± 0.36	1497.3 ± 406.7	71.8 ± 11.3
	40 nM Quinacrine	2.07 ± 0.15	1750.3 ± 492.4	57.7 ± 11.4
	40 nM Orlistat	2.13 ± 0.06	1093.4 ± 423.0	76.2 ± 27.9
	40 nM EGCG	1.96 ± 0.19	1402 .1 ± 446.2	61.6 ± 10.1
	4 nM SB202190	1.37 ± 0.58	1049.8 ± 518.1	45.7 ± 28.5
	4 nM SB202190 (exponential addition)	1.76 ± 0.12	1410.9 ± 724.8	60.9 ± 18.9
N. oculata	Control	1.90 ± 0.11	328.5 ± 125.7	48.2 ± 11.9
	DMSO (0.4%)	1.78 ± 0.06	390.7 ± 102.0	67.2 ± 7.8
	4 nM Forskolin	2.10 ± 0.18	344.9 ± 76.8	88.7 ± 23.8
	400 nM cAMP	2.00 ± 0.26	260.7 ± 14.0	72.7 ± 14.1
	400 nM Quinacrine	2.05 ± 0.22	482.1 ± 239.6	73.0 ± 14.3
	4 μM EGCG	1.93 ± 0.17	331.4 ± 49.5	67.9 ± 23.6
N. salina	Control	1.20 ± 0.11	350.1 ± 209.5	65.1 ± 10.5
	DMSO (0.4%)	1.31 ± 0.23	373.2 ± 154.6	81.3 ± 11.6
	4 μM cAMP	1.47 ± 0.17	327.7 ± 29.1	91.9 ± 28.6
	40 nM Quinacrine	1.17 ± 0.05	254.3 ± 30.2	66.7 ± 6.6
	40 μM EGCG	1.35 ± 0.12	364.1 ± 106.7	76.7 ± 15.1
	4 μM EGCG (in water)[c]	1.07 ± 0.21	284.3 ± 49.4	92.0 ± 16.2
	40 nM propyl gallate	1.17 ± 0.10	496.9 ± 325.5	105.0 ± 15.6
	4 nM BHA	1.12 ± 0.03	391.7 ± 137.1	102.6 ± 11.2
P. tricornutum	Control	0.84 ± 0.19	348.8 ± 122.9	51.7 ± 19.5
	DMSO (0.4%)	0.81 ± 0.19	279.6 ± 151.6	55.4 ± 19.8
	76 pM Gossypol	0.83 ± 0.16	286.3 ± 41.7	70.6 ± 17.0
	40 nM cAMP	0.96 ± 0.06	429.1 ± 95.8	71.2 ± 14.1
	120 nM AICAR	0.88 ± 0.08	357.8 ± 66.6	80.7 ± 10.3
	4 μM EGCG (in water)[c]	0.80 ± 0.33	339.6 ± 139.0	59.2 ± 28.4

[a]Comparison of dry weight and lipid extracts for 500-mL microalgae cultures treated with bioactive small molecules vs control cultures with and without DMSO. All cultures were performed with three or more replicates unless otherwise indicated. All data indicates the average with the standard deviation denoted. [b]Biomass refers to the recovered dry biomass from individual culture growth experiments used for the extraction. [c]Two replicates performed.

V. TAG Analysis

Analysis of microalgal lipid extracts using ^{1}H NMR Spectroscopy. Dried lipid extract was dissolved in 650 μL of deuterated chloroform ($CDCl_3$) with the addition of approximately 5 mg of 3,4,5-trichloropyridine (Alfa Aesar, Ward Hill, MA) as an internal standard, and then transferred to a 5-mm NMR tube. ^{1}H NMR spectra were acquired at 283 K on a 300, 400 or 600 MHz NMR spectrometer (Varian, Palo Alto, CA) for 16 scans with a relaxation delay of 1 s, pulse angle of 45 degrees, and line broadening of 0.2 Hz. Samples were referenced to tetramethylsilane at 0.00 ppm and 3,4,5-trichloropyridine at 8.53 ppm (singlet). Figures were processed using MestReNova software (version 5 or 7, Mestrelab Research, Spain) **(Fig. S10)**. Peak assignment of fatty acids and their derivatives are based on NMR spectroscopic studies of previously reported algal lipid extracts.[11,12]

Preparation of TAGs for MALDI-TOF analysis using solid-phase extraction. For MALDI-TOF analysis, triacylglycerols were prepared using solid-phase extraction (SPE) with silica SPE cartridges (500 mg, Silicycle, Quebec) to remove chlorophyll. The nonpolar extract was dissolved in 300 μL hexanes, and loaded onto an SPE cartridge primed with hexanes. A mixture of 80:20:1 (v/v/v) hexanes/diethyl ether/acetic acid was used as mobile phase to elute the TAGs.[13] SPE removes all chlorophyll in this process. A residual polar fraction containing polar lipids and chlorophyll was obtained by elution with acetone. All extracts and TAG fractions were dried under vacuum and stored under argon in amber vials at -20°C before spectroscopic analysis (^{1}H NMR spectroscopy or MALDI-TOF mass spectrometry).

MALDI-TOF MS analysis of microalgal lipid extracts. All MALDI-TOF MS spectra were acquired on an Applied Biosystems 4700 MALDI-TOF-TOF mass spectrometer (Foster City, CA) with internal MALDI source, a 355-nm pulsed Nd:YAG laser, and was operated in positive ionization mode for analysis. The TOF was in Reflectron mode with laser intensity from 5500-6500 *Volts*. Each acquisition consisted of 2500 shots with a focus mass of 900 Da, and a scan range of m/z 400-1100. Multiple acquisition scans were performed at different laser intensities to determine optimal conditions. Samples for the MALDI-TOF were diluted to 5 mg/mL in hexane, and spotted in the fast-evaporation method in a 1:2 ratio with DHB (2,5-dihydroxybenzoic acid) as the matrix. Re-spotting with methanol allowed for the matrix and sample to mix without hexane interactions, and allowed for better crystal formation. All samples on MALDI plate were allowed to dry before MS analysis. Data was normalized to base peak in all cases (**Figs. S11** and **S12)**.

Transesterification of TAGs to Fatty Acid Methyl Esters (FAMEs) monitored by TLC, GC/MS and ^{1}H NMR analysis. After the initial weight was recorded, the nonpolar extract set aside for transesterification was dissolved in 3.0 mL of 0.6 M sulfuric acid in methanol and stirred vigorously at 60 °C for 45 minutes according to previously reported procedures.[14-16] Reaction progress was monitored by thin layer chromatography (TLC). After cooling to room temperature, the reaction was neutralized (saturated aqueous sodium bicarbonate), extracted (hexanes), and the organic layer was isolated and concentrated *in vacuo*, yielding FAMEs and any unconverted lipids. The aqueous layer was discarded. The conversion of several transesterification reactions was also monitored using ^{1}H NMR spectroscopy, where conversion was determined by the presence of methyl ester proton signal at 3.67 ppm. The sample was concentrated and reconstituted in methanol for GC/MS analysis to a final concentration of 2.5 mg/mL. 5 μL of sample was injected via split-less injection. The temperature program for

GC/MS used an initial temperature of 50°C and a final temperature of 200°C, with a rate of 2.5 ˚C increase per minute to utilize a one-hour analysis period for optimal FAME peak separation.

Analysis of compound cost for commercial applications. To assess the industrial viability of using chemical triggers for growing microalgae in a large-scale pond, we calculated the cost of several lead compounds for a 50,000 L pool size (Table S6). While epigallocatechin gallate (EGCG) is not a competitively-priced molecule for industrial applications, this initial screening result led us to identify propyl gallate and BHA, which exhibit similar lipid increases and are dramatically more affordable on a large scale. Also, since biological activity is observed using water delivery for several compounds, the costly addition of DMSO can be avoided. The pricing for 0.04% of DMSO is also indicated in Table S6. In general for larger cultures, it is envisioned that the overall amount of DMSO could be decreased ten-fold using the addition of a more concentrated DMSO stock solution and water-soluble compounds can be added without DMSO.

Table S6. Cost to dose a 50,000 L pond of microalgae with optimal compound concentration

Compound	Price/gram[a]	Optimal concentration identified in screening[d]	Desired concentration (M)	MW (g/mol)	Amount needed	Price for 50,000 L pool
EGCG	$1,200.00[b]	4 μM	4.00E-06	458.40	91.68 g	$110,016.00
cAMP	$107.00	4 μM	4.00E-06	329.20	65.84 g	$7,044.88
Forskolin	$4,950.00[c]	4 nM	4.00E-09	410.50	0.0821 g	$406.40
BHA	$0.06	4 nM	4.00E-09	180.24	0.036 g	$0.002
Propyl gallate	$0.09	40 nM	4.00E-08	212.20	0.4244 g	$0.04
DMSO	$64.16/L	0.04%	--	--	20 L	$1,283.20

[a]Unless otherwise indicated, the price per gram for each compound is based on the direct comparison of pricing from Fisher Scientific or Sigma Aldrich without academic discounts, whichever company provided a more cost-effective pricing for larger scale quantities (e.g. in some cases up to 10 Kg). [b]Based on pricing from Axxora for 50 mg. [c]Based on pricing from AK Scientific for 100 mg. [d] Optimal concentration values are based on results with *N. salina*, with the concentrations of forskolin based on results with *N. oculata*.

VI. NMR and MALDI-TOF Spectra

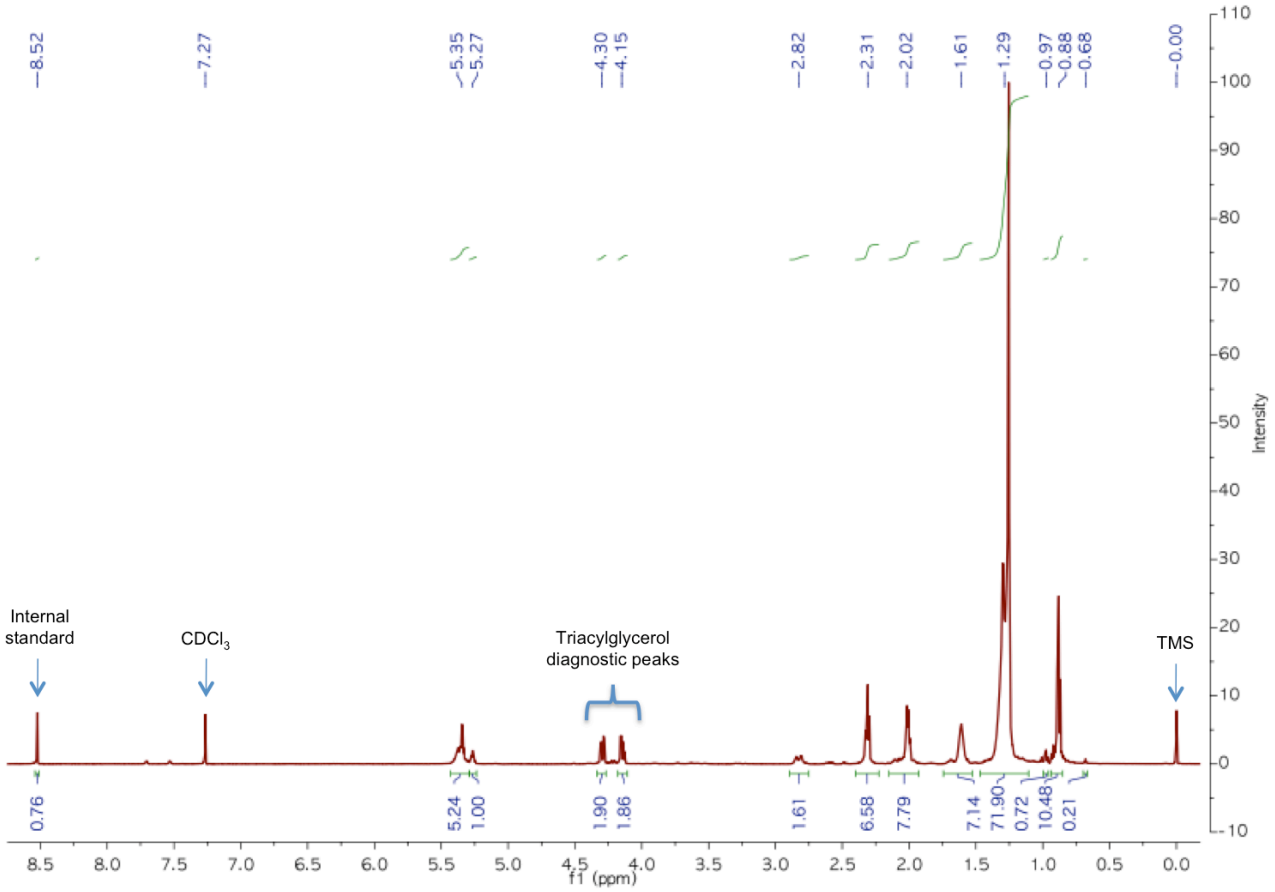

Figure S10. Example of ^{1}H NMR spectra of algae lipid extract for *N. salina*. Spectra were acquired on a Varian 600 MHz NMR spectrometer at 294 K for 16 scans with a relaxation delay of 1 s, pulse angle of 45 degrees, and line broadening of 0.2 Hz. Samples were referenced to tetramethylsilane at 0.00 ppm and 3,4,5-trichloropyridine at 8.52 ppm. Triacylglycerol peaks at 5.27, 4.30, and 4.15 ppm serve as diagnostic peaks for determining lipid extract purity and composition.

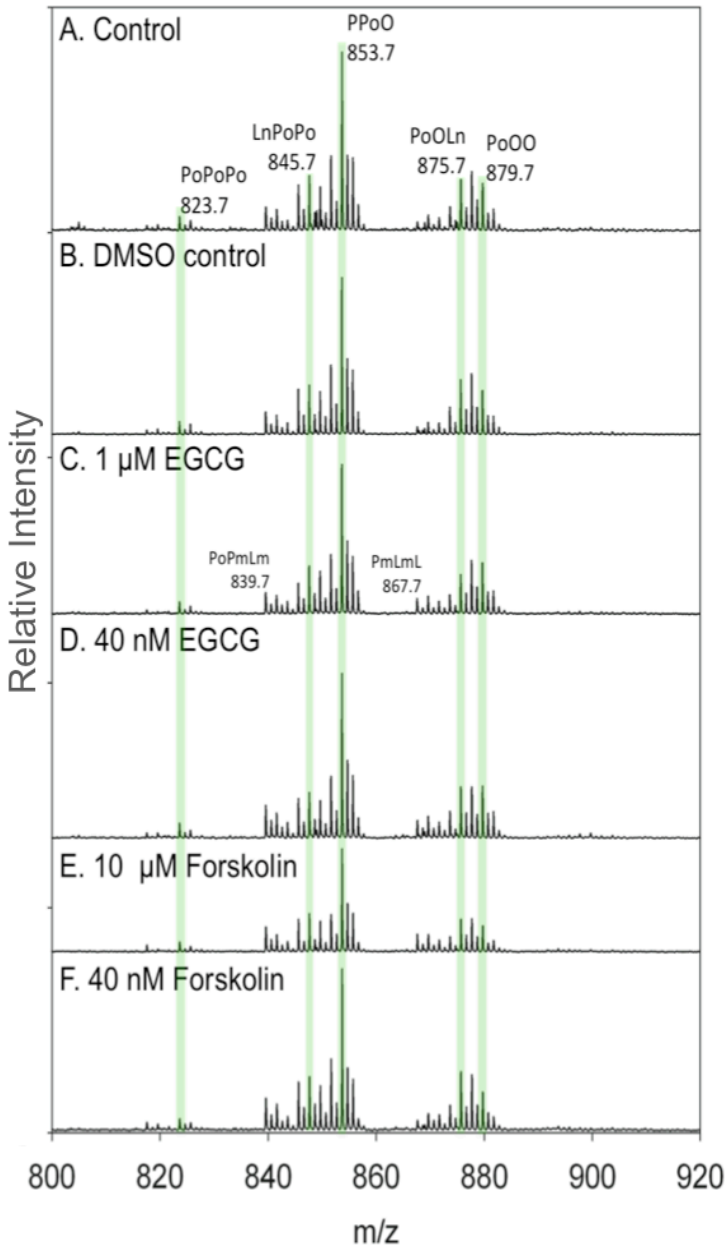

Figure S11. MALDI-TOF analysis of TAG extracts from chemical genetic batch culture experiments for *Nannochloris sp.* investigating compound effect on fatty acid saturation and chain length. A 500-mL culture of *Nannochloris sp*. with their perspective compounds starting at Day 0 and grown to 3 days into stationary phase before lipid extraction. No large differences in the TAG profile are detected. Highlighted sections were used to help compare and monitor the same peaks indicating the type of fatty acid in each culture.

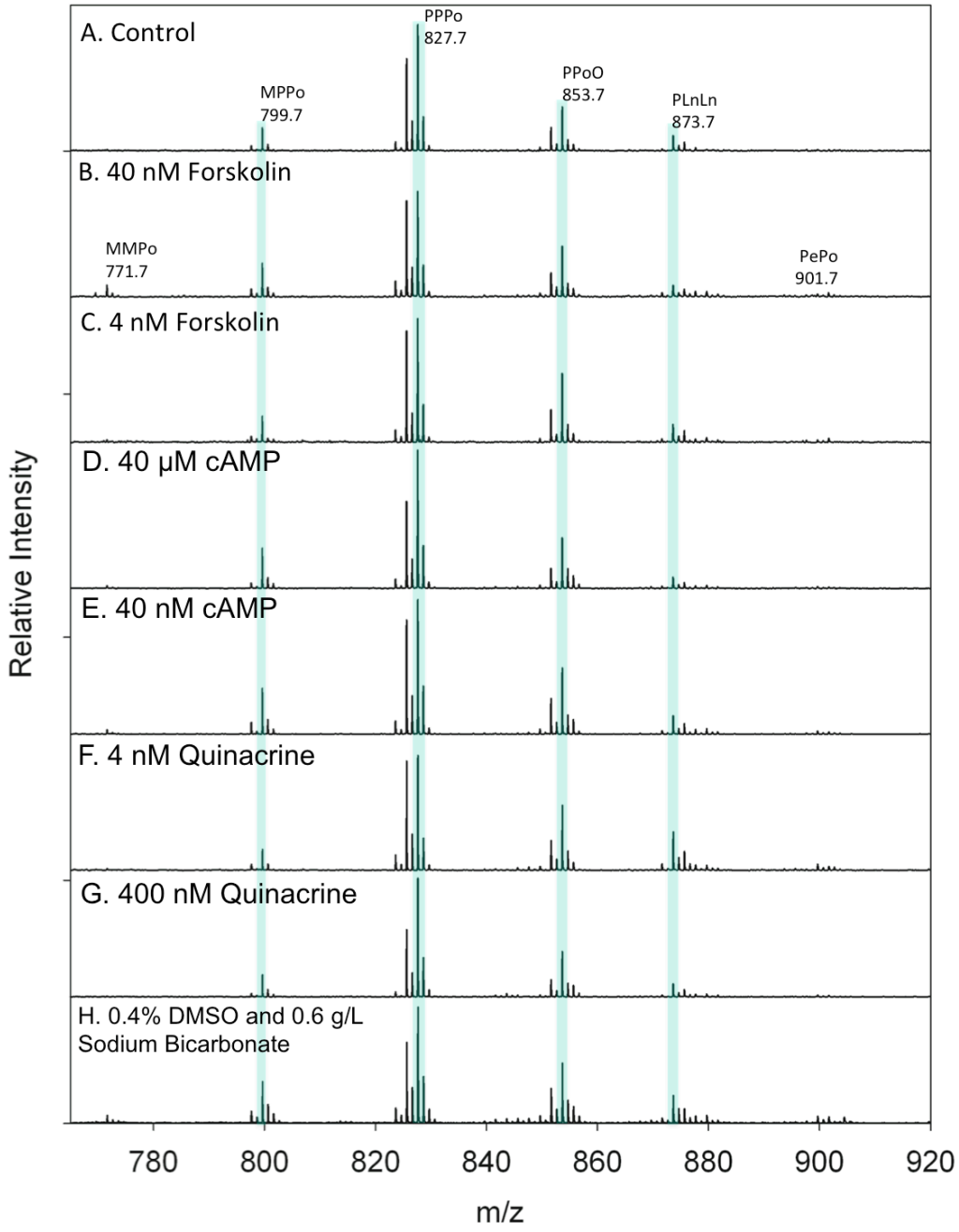

Figure S12. MALDI-TOF analysis of TAG extracts from chemical genetic batch culture experiments for *N. oculata* investigating compound effect on fatty acid saturation and chain length. No significant differences in saturation or chain length detected. Highlighted sections were used to help compare and monitor the same peaks indicating the type of fatty acid in each culture.

References

1. Chen, W., Zhang, C., Song, L., Sommerfeld, M., and Hu, Q. (2009) A high throughput Nile red method for quantitative measurement of neutral lipids in microalgae, *J. Microbiol. Meth. 77*, 41-47.
2. Pick, U., and Rachutin-Zalogin, T. (2012) Kinetic anomalies in the interactions of Nile red with microalgae, *J. Microbiol. Meth. 88*, 189-196.
3. Cooper, M. S., Hardin, W. R., Petersen, T. W., and Cattolico, R. A. (2010) Visualizing "green oil" in live algal cells, *J. Biosci. Bioeng. 109*, 198-201.
4. Bligh, E. G., and Dyer, W. J. (1959) A Rapid Method of Total Lipid Extraction and Purification, *Can. J. Biochem. Physiol. 37*, 911-917.
5. Folch, J., Lees, M., and Sloane Stanley, G. H. (1957) A simple method for the isolation and purification of total lipides from animal tissues, *J. Biol. Chem. 226*, 497-509.
6. Lee, J.-Y., Yoo, C., Jun, S.-Y., Ahn, C.-Y., and Oh, H.-M. (2010) Comparison of several methods for effective lipid extraction from microalgae, *Bioresour. Technol. 101*, S75-S77.
7. Guckert, J., Cooksey, K., and Jackson, L. (1988) Lipid sovent systems are not equivalent for analysis of lipid classes in the microeukaryotic green alga, *Chlorella*, *J. Microbiol. Meth. 8*, 139-149.
8. Iverson, S., Lang, S., and Cooper, M. (2001) Comparison of the bligh and dyer and folch methods for total lipid determination in a broad range of marine tissue, *Lipids 36*, 1283-1287.
9. Cooney, M., Young, G., and Nagle, N. (2009) Extraction of Bio-oils from Microalgae, *Sep. Purif. Rev. 38*, 291-325.
10. Levasseur, M., Thompson, P.A., and Harrison, P.J. (1993). Physiological Acclimation of Marine Phytoplankton to Different Nitrogen Sources. *J. Phycol. 29*, 587–595.
11. Pollesello, P., Toffanin, R., Murano, E., Paoletti, S., Rizzo, R., and Kvam, B. (1992) Lipid extracts from different algal species: ^{1}H and ^{13}C-NMR spectroscopic studies as a new tool to screen differences in the composition of fatty acids, sterols and carotenoids, *J. Appl. Phycol. 4*, 315-322.
12. Danielewicz, M. A., Anderson, L. A., and Franz, A. K. (2011) Triacylglycerol profiling of marine microalgae by mass spectrometry, *J. Lipid Res. 52*, 2101-2108.
13. Picariello, G., Paduano, A., Sacchi, R., and Addeo, F. (2009) MALDI-TOF Mass spectrometry profiling of polar and nonpolar fractions in heated vegetable oils, *J. Agric. Food. Chem. 57*, 5391-5400.
14. Freedman, B., Pryde, E., and Mounts, T. (1984) Variables affecting the yields of fatty esters from transesterified vegetable oils, *J. Am. Oil Chem. Soc. 61*, 1638-1643.
15. Antolín, E. M., Delange, D. M., and Canavaciolo, V. G. (2008) Evaluation of five methods for derivatization and GC determination of a mixture of very long chain fatty acids (C24:0–C36:0), *J. Pharm. Biomed. Anal. 46*, 194-199.
16. Sathish, A., and Sims, R. C. (2012) Biodiesel from mixed culture algae via a wet lipid extraction procedure, *Bioresour. Technol. 118*, 643-647.